

ORIGINAL ARTICLE

TIMP3 controls cell fate to confer hepatocellular carcinoma resistance

V Defamie¹, O Sanchez², A Murthy¹ and R Khokha¹

Inflammation enables human cancers and is a critical promoter of hepatocellular carcinoma (HCC). TIMP3 (Tissue inhibitor of metalloproteinase 3), a natural metalloproteinase inhibitor, controls cytokine and growth factor bioavailability to keep inflammation in check and regulate cell survival in the liver. TIMP3 is also found silenced in human cancers. We therefore tested whether *Timp3* affects HCC predisposition. Remarkably, genetic loss of *Timp3* protected from carcinogen-induced HCC through the immediate engagement of several tumor suppressor pathways, while tumor necrosis factor (TNF) signaling was dispensable for this protection. All wild-type mice developed HCC by 12 months, whereas HCC incidence was reduced to 33% at 12 months and 57% at 15 months in *Timp3* null mice. Upon acute carcinogen treatment the deficient livers exhibited greater cytokine expression, but lower cell death and higher hepatocyte senescence. We found that precocious activation of p53, p38 and Notch preceded senescence and hepatic cell differentiation, and these events were conserved throughout tumorigenesis. *Timp3*-deficient mouse embryo fibroblasts also responded to carcinogen by favoring senescence over apoptosis. We conclude that *Timp3* status determines p53, p38 and Notch coactivation to instruct hepatic cell fate and transformation and uncover mechanisms that are protective even within a pro-inflammatory microenvironment.

Oncogene (2015) 34, 4098–4108; doi:10.1038/onc.2014.339; published online 27 October 2014

INTRODUCTION

Chronic liver damage during hepatitis and cirrhosis is a key contributing factor to hepatocellular carcinoma (HCC) usually associated with alcoholism, hepatitis B or C viral infection, and aflatoxin B1 consumption.^{1–3} Diabetes and non-alcoholic steatohepatitis are new etiological factors in liver cancer.⁴ The increasing incidence of these diseases in developed countries is exposing more populations to the risk of developing HCC. Malignant transformation of hepatocyte involves the perpetuation of a wound-healing response triggered by parenchymal cell death and compensatory regeneration in the context of inflammation and oxidative DNA damage. The tumor suppressor p53 is immediately recruited upon DNA damage and dictates hepatocyte cell fate. In addition, the mitogen-activated protein kinase (MAPK) p38 as well as Notch have been suggested to provide tumor-suppressive function in the liver.^{5,6} However, activation of these critical genes by microenvironmental factors during inflammation remains poorly understood. The extracellular tissue inhibitor of metalloproteinase 3 (TIMP3) has a fundamental role in liver biology. Studies pertinent to hepatic fate such as liver regeneration,⁷ systemic inflammation,⁸ Fas-dependent hepatotoxicity⁹ and high-fat diet-induced diabetes¹⁰ or steatohepatitis¹¹ have identified TIMP3 to be a critical regulator of hepatic inflammation, cell death and survival. A key function of TIMP3 is to inhibit ADAM17 (a disintegrin and metalloproteinase 17), a protease responsible for ectodomain shedding of multiple cell surface proteins including tumor necrosis factor (TNF), TNF receptors and epidermal growth factor (EGF) receptor ligands, or participating in Notch cleavage.^{12–14} Thus, TIMP3 regulates TNF and EGF signaling, and possibly the Notch activation.^{7,9,15} Genomic studies have identified TIMP3 silencing in several human cancers via hypermethylation,^{16,17} microRNA^{18,19} and loss of heterozygosity,^{20,21} suggesting a tumor-suppressive function for this gene.

Timp3-deficient mouse offered an opportunity to model liver tumorigenesis in the context of inflammation and TIMP3 silencing.

Contrary to our expectation, we found that TIMP3 is required for liver tumorigenesis. *Timp3*-deficient mice were strongly resistant to carcinogen-induced HCC despite their proclivity for inflammation. The loss of *Timp3* enabled coactivation of p53, p38 and Notch signaling enhancing senescence and hepatic cell differentiation. The TNF pathway participated in progression to malignancy but was not essential for HCC. In conclusion, TIMP3 has a critical role in liver tumorigenesis by directing the balance between hepatocyte apoptosis and senescence during the p53-dependent DNA damage response.

RESULTS

Heightened inflammation but compromised hepatic cell death in carcinogen-treated *Timp3*^{-/-} mice

An acute dose of the carcinogen diethylnitrosamine (DEN; 100 µg/g body weight) administered to mice (Figure 1a) triggers immediate hepatocyte DNA damage and cell death, with concomitant Kupffer cell activation releasing cytokines as hepatomitogens.²² DEN cytotoxicity depends on its metabolic activation by cytochrome P450 2E1 (CYP2E1) within centrolobular hepatocytes;²³ *Cyp2e1*^{-/-} mice are resistant to DEN-induced HCC.²⁴ We performed quantitative reverse transcription PCR measurements over 48 h post DEN and found comparable *Cyp2e1* expression between *Timp3*^{-/-} and wild-type (WT) livers, thereby suggesting similar DEN-induced cytotoxicity in these groups (Figure 1b). Participation of the *Timp* gene family members in DEN-induced hepatic response was assessed by measuring expression of individual *Timp1*, *Timp2*, *Timp3* and *Timp4* post DEN in WT liver. *Timp3* expression increased at 4 h and steadily declined over 24 h, indicating its

¹Ontario Cancer Institute, University of Toronto, Toronto, Ontario, Canada and ²University of Ontario Institute of Technology, Oshawa, Ontario, Canada. Correspondence: Dr R Khokha, MARS—Medical Discovery Tower, TMDT Research, 101 College Street, Toronto, Ontario, Canada M5G 1L7. E-mail: rkhokha@uhnres.utoronto.ca

Received 2 June 2014; revised 29 August 2014; accepted 4 September 2014; published online 27 October 2014

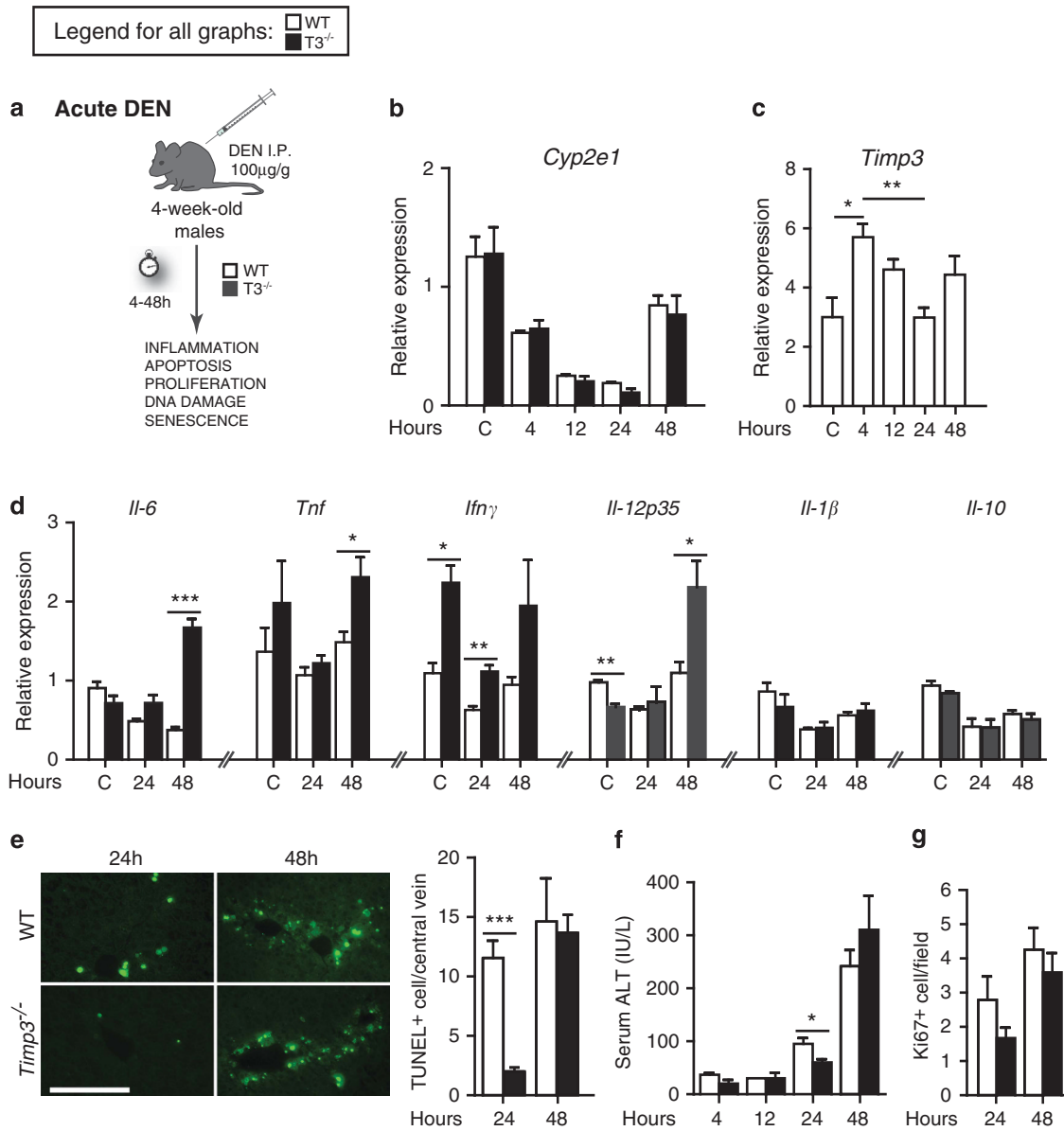


Figure 1. Cytokine expression and hepatocyte apoptosis after DEN-induced hepatic injury. **(a)** A schematic showing the analyses on 4-week-old male mice after acute DEN treatment. **(b)** Expression of *Cyp2E1*, the cytochrome responsible for DEN metabolism, determined by reverse transcription PCR (RT-PCR). **(c)** RT-PCR measurement of *Timp3* expression in WT liver post DEN. **(d)** Hepatic cytokine expression in DEN- or PBS-treated control (C) WT and *Timp3*^{-/-} mice as determined by RT-PCR. **(e)** Representative images of TUNEL staining in the indicated mouse cohorts and quantification of the positive hepatocytes (green) undergoing apoptotic cell death post DEN. **(f)** Serum level of ALT reflecting hepatic injury. **(g)** Quantification of hepatocytes proliferation identified by Ki67 immunostaining. Data are presented as the mean ± s.e.m., *n* = 3–6 mice per group. **P* < 0.05, ***P* < 0.01 and ****P* < 0.001 for the indicated comparisons. Scale bar, 100 μm.

specific induction at the onset of the hepatic carcinogen challenge, whereas other *Timps* did not show modulation at the early time points (Figure 1c and Supplementary Figure S1). All *Timps*, except *Timp4*, then rose at 48 h although not significantly. Measurement of gene expression in pro-inflammatory cytokines interleukin (IL)-6, TNF, interferon gamma (IFN γ) and IL-12p35 showed a greater increase in *Timp3*^{-/-} versus WT livers, whereas the levels of IL-1 β and IL-10 (an anti-inflammatory cytokine) remained similar (Figure 1d). Measurement of IL-6, TNF α and IFN γ protein levels by enzyme-linked immunosorbent assay in liver tissue lysates confirmed the changes observed at RNA level (Supplementary Figure S2).

DEN products cause DNA damage by forming DNA ethyl adducts and this is typically followed by cell death and

compensatory hepatocyte proliferation. Hepatocyte apoptosis was determined by the terminal deoxynucleotidyl transferase dUTP nick end labeling (TUNEL) assay and cleaved caspase 3 immunohistochemistry (IHC), proliferation was assessed by Ki67 IHC, and the release of alanine transaminase (ALT) into serum provided another measure of hepatic damage over 48 h following carcinogen administration. We observed that hepatocyte cell death was reduced despite the heightened liver inflammation in *Timp3*^{-/-} liver. Specifically, far fewer apoptotic hepatocytes were detected at 24 h post DEN (TUNEL and cleaved caspase 3-positive cells (Figure 1e and Supplementary Figure S3)), and ALT levels were lower compared with WT (Figure 1f). Hepatocyte proliferation was marginally lower at this time point (Figure 1g). However, these parameters of liver injury were comparable at 48 h,

suggesting an altered kinetics of cellular response to DNA damage in the *Timp3* null liver. Therefore, TIMP3 not only altered hepatic inflammatory response but also hepatocyte cell death upon genotoxic insult.

Increased p53 activation in *Timp3* null hepatocytes

In response to cellular stress such as the DNA damage, p53 activation promotes cell cycle checkpoints, DNA repair, cellular apoptosis and senescence. Histone gamma H2AX phosphorylation (γ -H2AX) is an immediate event in DNA damage and repair,²⁵ and γ -H2ax foci seen in WT hepatocytes at 4 h were mostly resolved by 12 h post DEN (Figure 2a). Equivalent at 4 h, these foci remained obvious until 12 h in *Timp3*^{-/-} centrolobular hepatocytes indicating an early difference in the DNA damage response. Examination of p53 in hepatocyte nuclei by IHC showed fourfold higher number of p53-positive nuclei at 12 h in the null liver reflecting a more robust p53 response, whereas WT livers displayed a transient peak of nuclear p53 localization at 24 h (Figure 2b). Western blotting confirmed early p53 activation and higher levels in *Timp3*^{-/-} liver (Figure 2c). We determined the expression of several p53 target genes, and those involved in p53 regulation (*Mdm2*) and cycle arrest (*p21*) were significantly higher at 4 h in deficient liver, whereas pro-apoptotic genes (*Puma* and *Noxa*) were lower than WT throughout the time course, providing an explanation for the delayed cell death observed in carcinogen-challenged *Timp3*^{-/-} liver (Figure 2d). Thus, differential p53 kinetics directed the DNA damage response; p53 activation normally favors apoptosis in WT liver, but precocious p53 activity, defect in apoptosis and p21 upregulation suggested increased cell cycle arrest in liver lacking the *Timp3* gene.

The *Timp3* null cells are predisposed to senescence

Given the higher p53 activity but lower hepatocyte apoptosis, we then examined cellular senescence by comparing p21 protein level and senescence-associated β -galactosidase activity (SA- β -gal) after acute DEN treatment. p21 levels were higher as early as 4 h, and increased SA- β -gal staining was evident in deficient livers compared with WT controls (Figures 3a and b), raising the probability that precocious p53 activity has triggered cell cycle arrest and senescence in TIMP3 null liver. To assess whether *Timp3* loss promotes DNA damage-induced senescence in a cell type other than hepatocytes, low-passage mouse embryo fibroblasts (MEFs) were exposed to methyl methanesulfonate (MMS; 130 μ g/ml, 2 h). The alkylating agent MMS was chosen for induction of DNA damage in cell culture setting, as it does not require cytochrome P450-mediated hepatic metabolism unlike DEN. After MMS treatment, the cells were allowed to recover in fresh media for 0–48 h (Figure 3c). *Timp3*^{-/-} MEFs responded with higher expression of p21 within the first 4 h (Supplementary Figure S4) and substantially lower apoptosis compared with WT cells (Figure 3d). In fact level of cleaved caspase 3 at 48 h in null MEFs was comparable to those at 4 h in WT revealing the magnitude of cell death delay. Furthermore, senescence-associated protein p16 expression was sustained over 48 h in *Timp3*^{-/-} MEFs (Figure 3d). Higher SA- β -gal staining was seen from 0 to 24 h following MMS treatment in TIMP3-deficient cells (Figure 3e). These results show that TIMP3 alters the balance between apoptosis and senescence following DNA damage in diverse cell types such as hepatocytes and fibroblasts.

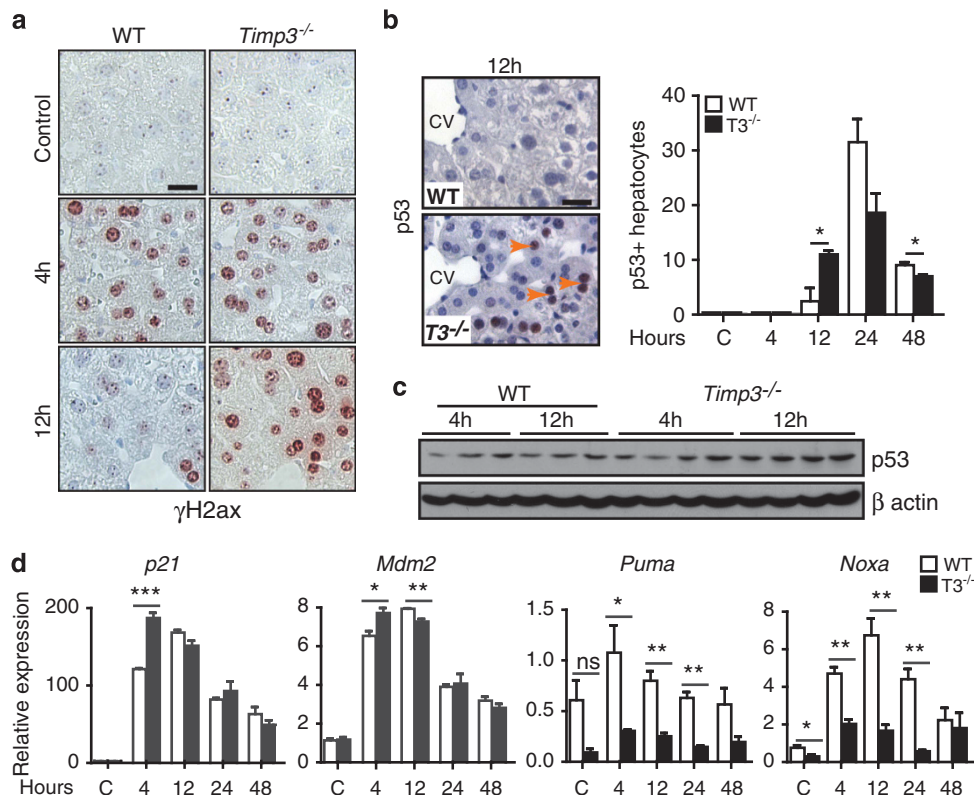


Figure 2. p53 activation after acute DEN treatment. (a) Representative images of immunostaining for histone γ H2ax, a marker of DNA damage and repair following acute DEN treatment (100 mg/kg), $n=3-4$ mice per group. (b) p53 immunostaining and quantification of positive hepatocyte nuclei (arrows) around the central veins (CVs) at 12 h post DEN. WT, $n=3$; *Timp3*^{-/-}, $n=4$. (c) Immunoblotting of p53 at 4 and 12 h post DEN in liver protein extracts. Each lane represents an individual mouse, and β -actin serves as a loading control. (d) Expression of p53 target genes within 48 h post DEN, as assessed by reverse transcription PCR. Data are presented as the mean \pm s.e.m. $n=3-4$ mice per group. Scale bar, 20 μ m. NS, not significant, * $P < 0.05$, ** $P < 0.01$ and *** $P < 0.001$ for the indicated comparisons.

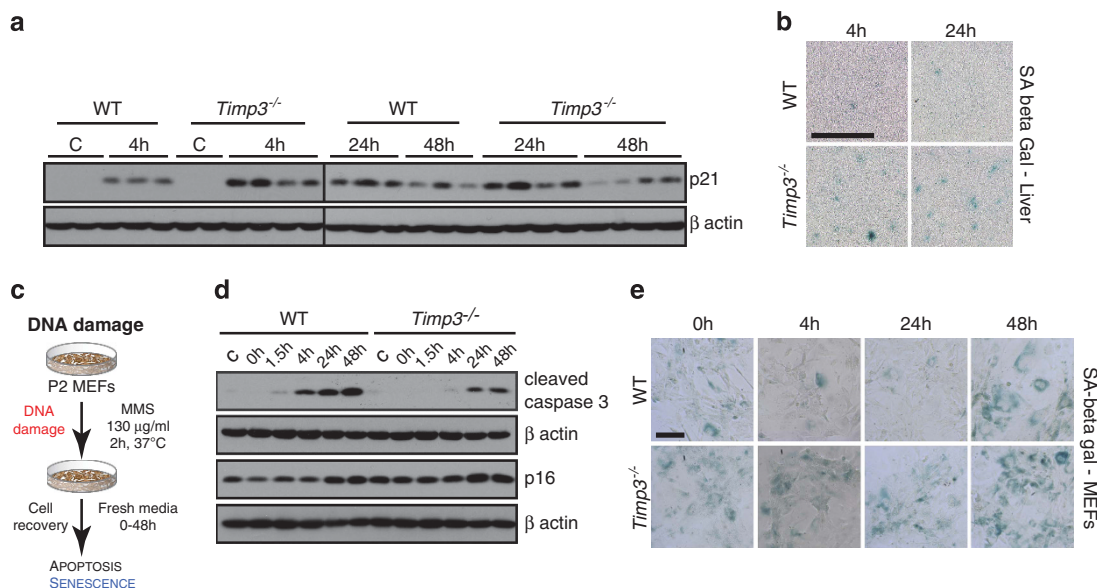


Figure 3. Measure of senescence in the *Timp3* null state. **(a)** Immunoblotting for p21 at the indicated times and genotypes. Each lane represents a mouse and β -actin serves as a loading control. **(b)** Representative images of senescence-associated β -galactosidase activity (SA- β -gal) highlighting the senescent cells in blue at 4 and 24 h post DEN. $n = 3$ mice per group. Scale bar, 100 μ m. **(c)** WT and *Timp3*^{-/-} low-passage MEFs were treated with methyl methanesulfonate (MMS; 130 μ g/ml for 2 h at 37 °C) to induce DNA damage and the media was replaced to allow cell recovery for the indicated time. **(d)** Immunoblotting of activated caspase 3 (cleaved caspase 3) and senescence related protein p16 in MEFs following MMS treatment and cell recovery. Untreated controls are marked as C. **(e)** Representative images of SA- β -gal activity highlighting the senescent MEFs in blue after MMS treatment and cell recovery at the indicated time points and genotypes. Scale bar, 200 μ m.

Timp3-deficient mice are protected from carcinogen-induced HCC. Hepatic inflammation is known to potentiate liver carcinogenesis but decreased hepatocyte apoptosis and/or increased senescence would impact the tumor initiation process. To study the importance of these opposing cellular events on HCC development, cohorts of WT and *Timp3*^{-/-} neonatal mice were given a single carcinogen injection (15-day-old males, 5 μ g/g of DEN), and tissue analyzed at 8 and 12 months post treatment (Figure 4a). DEN administration is a widely used method of inducing HCC, as it recapitulates many events seen in human liver cancer.²⁶ As expected, WT mice harbored large vascularized hepatic tumors by 12 months, with increased liver weight and serum ALT (Figures 4b–d). Tumorigenesis was markedly suppressed in *Timp3*^{-/-} mice as determined by lower tumor burden, tumor size and ALT levels, although the number of nodules on the liver surface was similar between the two cohorts (Figures 4b–f). Histological examination showed that all WT mice had HCC (100% incidence) by 12 months post DEN, but only 33% of the *Timp3*^{-/-} cohort developed HCC; the remaining *Timp3*^{-/-} mice had hepatoadenoma or hepatic cell damage (Table 1).

To establish whether *Timp3*^{-/-} mice were protected from liver carcinoma or merely delayed in developing cancer, a group of mice were aged and the tumor burden was examined at 15 months post DEN (Figures 4c–g). No significant increase in liver weight occurred between 12 and 15 months (Figure 4c), and the ALT levels were still severely reduced when compared with WT mice at 12 months (Figure 4d). More importantly, only 57% of the *Timp3*^{-/-} mice developed HCC, with the others harboring hepatoadenoma or foci (Table 1) indicating their prolonged resistance against carcinogen-induced liver tumorigenesis. This data provides strong evidence for TIMP3 requirement in HCC development.

HCC suppression is not dependent on TNF signaling

Molecular effectors of the nuclear factor- κ B pathway, activated downstream of TNF, are implicated in inflammation and liver cancer,^{22,27,28} although there is little understanding of how TNF

itself affects DEN-induced liver tumorigenesis. Cell surface release of TNF and its receptors is controlled by TIMP3, and many of the inflammation-related phenotypes of *Timp3*-deficient mice are rescued by deleting components of the TNF pathway.^{7–9} We tested whether HCC resistance requires TNF bioactivity by generating double knockouts that lacked TNF or TNF receptor I in addition to *Timp3* (*Timp3*^{-/-}/*Tnf*^{-/-}; *Timp3*^{-/-}/*Tnfr1*^{-/-}). At 12 months post DEN, TNF deficiency alone (*Tnf*^{-/-}) reduced the liver weight and tumor size compared with WT, but this difference was not statistically significant (Figures 5a and 4d). On the other hand, tumors classified as HCC were significantly lowered to 42%, suggesting TNF participation in malignant progression to HCC (Table 1). In contrast, compound cohorts *Timp3*^{-/-}/*Tnf*^{-/-} and *Timp3*^{-/-}/*Tnfr1*^{-/-} presented substantially greater tumor suppression than individual *Tnf* or *Timp3* knockouts. Specifically, tumor number and size were reduced, with liver weights being comparable to that of a normal, 12-month-old non-tumor bearing liver (WT = 1.33 \pm 0.04 $n = 6$; *Timp3*^{-/-}/*Tnf*^{-/-} = 1.36 \pm 0.3 $n = 5$; *Timp3*^{-/-}/*Tnfr1*^{-/-} = 1.39 \pm 0.20 $n = 9$; Figures 5a–d). Further, tumors classified as HCC fell to 25% in *Timp3*^{-/-}/*Tnf*^{-/-} and 11% in *Timp3*^{-/-}/*Tnfr1*^{-/-} groups (Table 1). The cumulative tumor inhibition seen in compound knockouts shows that TIMP3 and TNF act through different mechanisms to promote HCC. The process underlying HCC suppression in *Timp3*-deficient liver occurs despite excess inflammation observed at the onset of DNA damage.

p38 and Notch signaling aligns with p53 activation in the *Timp3* null state

We next ask how TIMP3, located in the extracellular microenvironment, can modulate the DNA damage response and hepatocyte cell fate after genotoxic stress. As MAPKs (p38, c-Jun NH(2)-terminal kinase (JNK) and extracellular signal-regulated kinase (ERK1/2)) can impact p53 activity and we previously found increased MAPK-dependent survival signaling during Fas-mediated cell death in *Timp3* null mice,⁹ we considered MAPKs as a protective mechanism.²⁹ Activation of these stress kinases

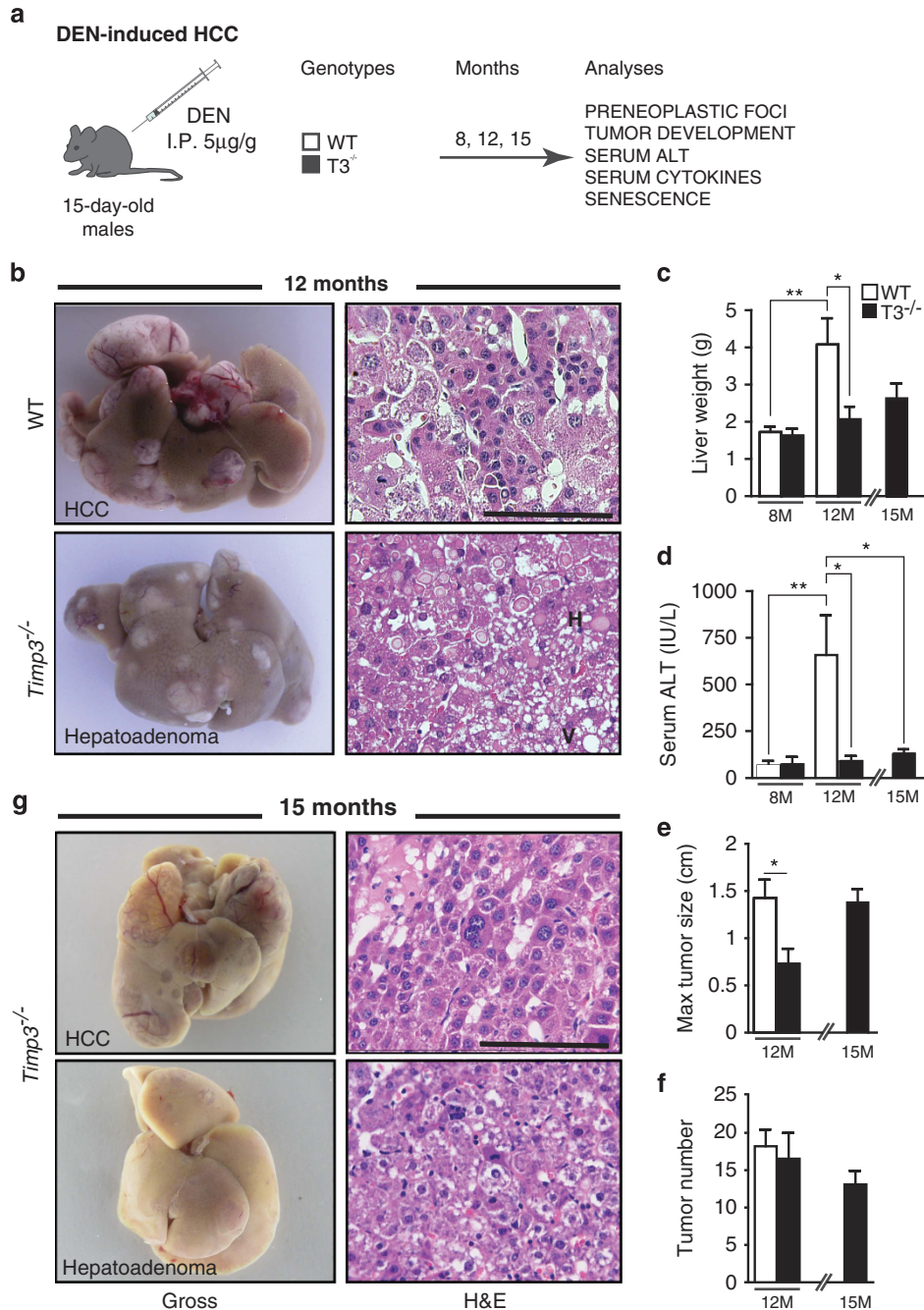


Figure 4. HCC development in WT and *Timp3*-deficient mice. **(a)** 15-Day-old male mice of mentioned were given a single injection of 5 µg/g of DEN, and liver tumorigenesis was examined 8, 12 and 15 months (M) later. **(b)** Macroscopic appearance and hematoxylin and eosin-stained sections of representative WT and *Timp3*^{-/-} livers at 12 months post DEN. Histology reveals well-differentiated HCC in WT liver, while *Timp3*^{-/-} liver shows hepatocellular adenoma and cell damage in the form of cytoplasmic hyaline (H) and vacuolar degeneration (V). **(c)** Liver weight at 8 (WT, *n* = 9; *Timp3*^{-/-}, *n* = 12), 12 (WT, *n* = 9; *Timp3*^{-/-}, *n* = 8) or 15 months (*n* = 7) post DEN. **(d)** Serum ALT levels at 8 (WT, *n* = 8; *Timp3*^{-/-}, *n* = 12), 12 (*n* = 5) or 15 months (*n* = 6). **(e)** Quantification of maximum tumor size; and **(f)** tumor number on the liver surface at 12 (*n* = 9) or 15 months (*n* = 7). **(g)** Macroscopic appearance and hematoxylin and eosin-stained sections of representative *Timp3*^{-/-} livers harboring HCC or hepatocellular adenoma at 15 months post DEN. Scale bars, 100 µm. Data are presented as the mean ± s.e.m. **P* < 0.05, ***P* < 0.01 for the indicated comparisons.

typically occurs in a wave, and we therefore examined p38, JNK and ERK1/2 phosphorylation over 48 h after acute DEN treatment. JNK and ERK1/2 activation in livers was generally comparable in *Timp3*^{-/-} and WT cohorts (Figure 6a and Supplementary Figure S5A). In contrast, the p38 phosphorylation kinetics was different between the two genotypes. A striking reduction in p38 phosphorylation noted in WT at 4 and 48 h was absent in

Timp3^{-/-} liver and p38 activation was sustained post DEN. Thus, TIMP3 deficiency allowed continued p38 MAPK signaling during hepatic damage.

TIMP3 is the endogenous inhibitor of ADAM17, a metalloproteinase critical for Notch signaling in the skin.³⁰ Notch coordinates biliary fate and bile duct morphogenesis in hepatic development,³¹ and has a complex role in HCC. ADAM17 and

Table 1. Histopathological analysis of liver tumors from DEN-treated mice

	12 Months					15 Months
	WT	<i>T3</i> ^{-/-}	<i>Tnf</i> ^{-/-}	<i>T3</i> ^{-/-} <i>Tnf</i> ^{-/-}	<i>T3</i> ^{-/-} <i>Tnfr1</i> ^{-/-}	<i>T3</i> ^{-/-}
Carcinoma	9/9 (100%)	3/9 (33%)	5/12 (42%)	1/4 (25%)	1/9 (11%)	4/7 (57%)
Adenoma	0/9	3/9	3/12	0/4	3/9	2/7
Foci	0/9	2/9	4/12	3/4	5/9	1/7
Normal liver	0/9	1/9	0/12	0/4	0/9	0/7

Abbreviations: DEN, diethylnitrosamine; *T3*^{-/-}, *Timp3*^{-/-}; WT, wild type. Liver sections obtained from the indicated genotypes at 12 and/or 15 months post-DEN injection (5 µg/g, 15-day-old males) were stained by hematoxylin and eosin, and the tumor were classified by a pathologist. The number of mice presenting HCC is also given as a percentage of the total number of mice analyzed.

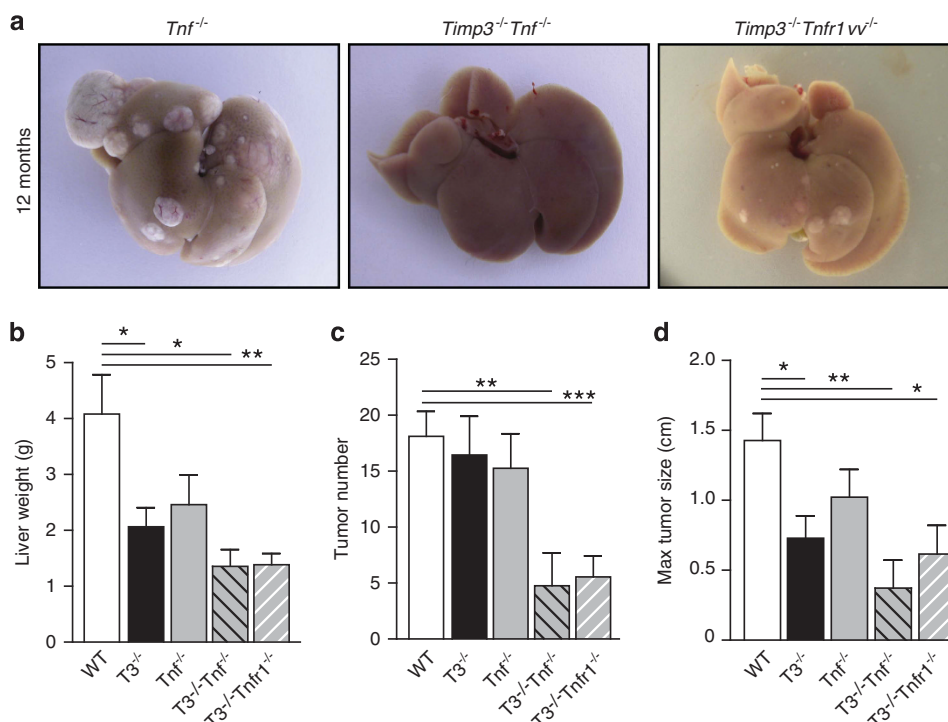


Figure 5. Consequence of TNF signaling defects on HCC development in *Timp*-deficient mice. **(a)** Gross liver images of the indicated genotypes at 12 months post DEN (5 µg/g, 15-day-old males). **(b)** Liver weight, **(c)** tumor number and **(d)** maximum tumor size on the liver surface of the indicated genotypes. Data are presented as the mean ± s.e.m. WT, *n* = 9; *Timp3*^{-/-}, *n* = 9; *Tnf*^{-/-}, *n* = 12; *Timp3*^{-/-}*Tnf*^{-/-}, *n* = 5; *Timp3*^{-/-}*Tnfr1*^{vvl-/-}, *n* = 9. **P* < 0.05, ***P* < 0.01 and ****P* < 0.001 for the indicated comparisons.

γ-secretase perform successive Notch cleavage to produce Notch intracellular domain (NICD) that then translocates to the nucleus and activate gene expression for cell fate determination. We found that NICD levels were higher in *Timp3*-deficient livers at 4 h post DEN (Figure 6b), and several liver-specific or ubiquitous Notch target genes were subsequently examined. SOX9 (SRX-box containing gene 9) and HNF1β (hepatocyte nuclear factor-1β) are transcriptional regulators of biliary development^{32,33} and both were elevated in *Timp3* null livers post DEN (Figure 6c). Interestingly, baseline SOX9 and HNF1β expression was also upregulated. On the other hand, expression of generic Notch targets, basic helix–loop–helix proteins Hes (Hairy enhancer of split) or Hey (Hairy-related family), did not differ between the two cohorts (Supplementary Figure S5B). The hepatocyte marker HNF4α was increased in *Timp3*^{-/-} liver³¹ (Figure 6c) and behaved similarly to SOX9 and HNF1β at baseline and 48 h. These data suggest that TIMP3 regulates Notch activation and subsequently affects hepatic cell differentiation.

Tumor suppressor coactivation triggers senescence and differentiation to attenuate HCC

Next, we focused on the preneoplastic stage (8 months post DEN) of liver tumorigenesis. WT foci exhibited extensive cellular damage and adjacent hepatic parenchyma compression, while *Timp3*^{-/-} foci conserved lobular architecture with the presence of portal triads and reduced hepatocyte damage (Figure 7a). Further, a lower proportion of Ki67-positive hepatocytes in *Timp3*^{-/-} foci (Figure 7b) indicated reduced proliferation. Serum IL-6, a potent hepatocyte mitogen,³⁴ was also lower at both 8 and 12 months in TIMP3 null mice, although serum TNF was similar (Figure 7c). In human HCC, the MKK6/p38 pathway is downregulated compared with the adjacent non-tumor tissues.³⁵ Comparison of p38 phosphorylation in tumor versus adjacent non-tumor tissues at 8 and 12 months in *Timp3*-deficient and WT groups was then performed (Figure 7d). We found increased p38 phosphorylation in tumor nodules at 8 months, and both non-tumor and tumor

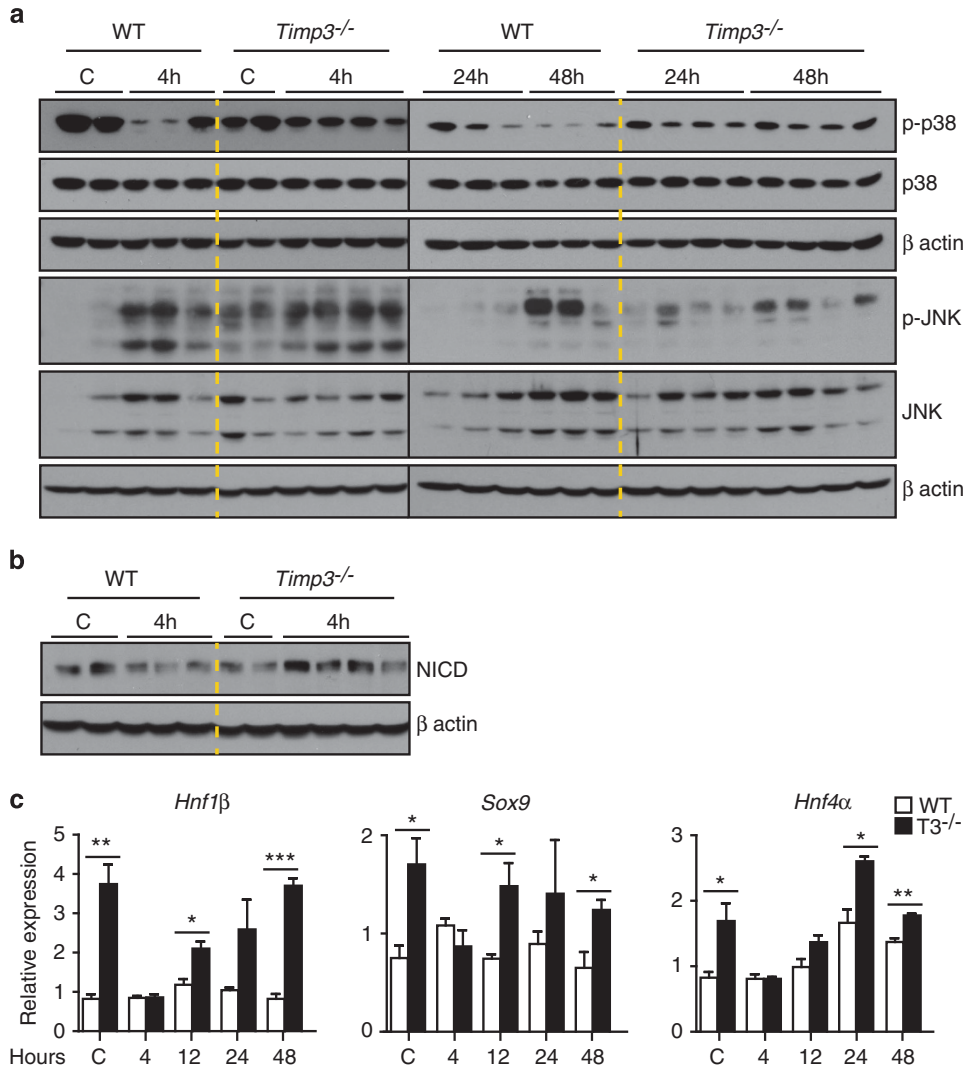


Figure 6. Kinetics of MAPK activation and Notch signaling after acute DEN treatment. **(a)** Comparison of activated p38 (p-p38) and JNK (p-JNK) kinases by immunoblotting in WT and *Timp3*^{-/-} liver at the indicated times post acute DEN treatment (100 μg/g, 4-week-old males). **(b)** Levels of Notch (NICD) in WT and *Timp3*^{-/-} livers extracts and in PBS-treated control mice (C). Each lane represents a mouse and β-actin serves as a loading control. **(c)** Cholangiocyte markers (*Sox9*, *Hnf1β*) and hepatocyte marker (*Hnf4α*) expression over 48 h in DEN-treated and control mice, as determined by reverse transcription PCR. Data are presented as the mean ± s.e.m. (*n* = 3). **P* < 0.05, ***P* < 0.01, and ****P* < 0.001 for the indicated comparisons.

tissue had higher p38 activation at 12 months in *Timp3*^{-/-} cohorts. With respect to Notch activation, NICD levels were also increased in the null liver at 8 months (Figure 7e). Moreover, Notch-dependent biliary specification transcription factors SOX9 and HNF1β were markedly higher, while hepatocyte marker HNF4α expression was not different (Figure 7f). Finally, a significant increase in p53 as well as the senescence-associated genes, p19 and p16, was found in preneoplastic *Timp3*-deficient livers (Figure 7g), indicating an increased propensity for prolonged cell cycle arrest and senescence over months of liver transformation in *Timp3*^{-/-} mice. Thus, p38 suppressor function and Notch-dependent hepatic cell differentiation cooperate to inhibit tumorigenesis in *Timp3* null mice.

DISCUSSION

A pro-inflammatory milieu is an essential component of human liver cancer development. Proteolytic overactivity, also critical for tumor progression, is found in all human cancers. Yet genetic loss of metalloproteinase inhibitor *Timp3* delays hepatic tumorigenesis

and prevents progression to malignancy despite eliciting heightened inflammation in response to carcinogen. We uncover a role of TIMP3 in p53, p38 and Notch co-regulation (Figure 7h). These signal transduction pathways are recruited during tumor suppression whereas TNF signaling is found dispensable. At the cellular level, *Timp3* loss shifts the carcinogen-induced DNA damage response to favor senescence and hepatic cell differentiation conferring protection against HCC.

Naugler *et al.*³⁶ showed that although DEN administration led to modest accumulation of TNF, ablation of TNFR1 had little effect on DEN-induced HCC. In contrary, another study suggested an important role for the TNF pathway in the promotion phase of HCC following administration of a choline-deficient and ethionine-supplemented diet to mice, as HCC development was attenuated in TNFR1-deficient mice.³⁷ Our data show that TNF is important in the process of liver tumorigenesis because DEN-induced HCC incidence was reduced in *Tnf*^{-/-} mice. Further, when the TNF pathway was deleted through removal of this ligand or its receptor in combination with TIMP3, the extent of HCC resistance was more profound. We hypothesize that TNF promotes

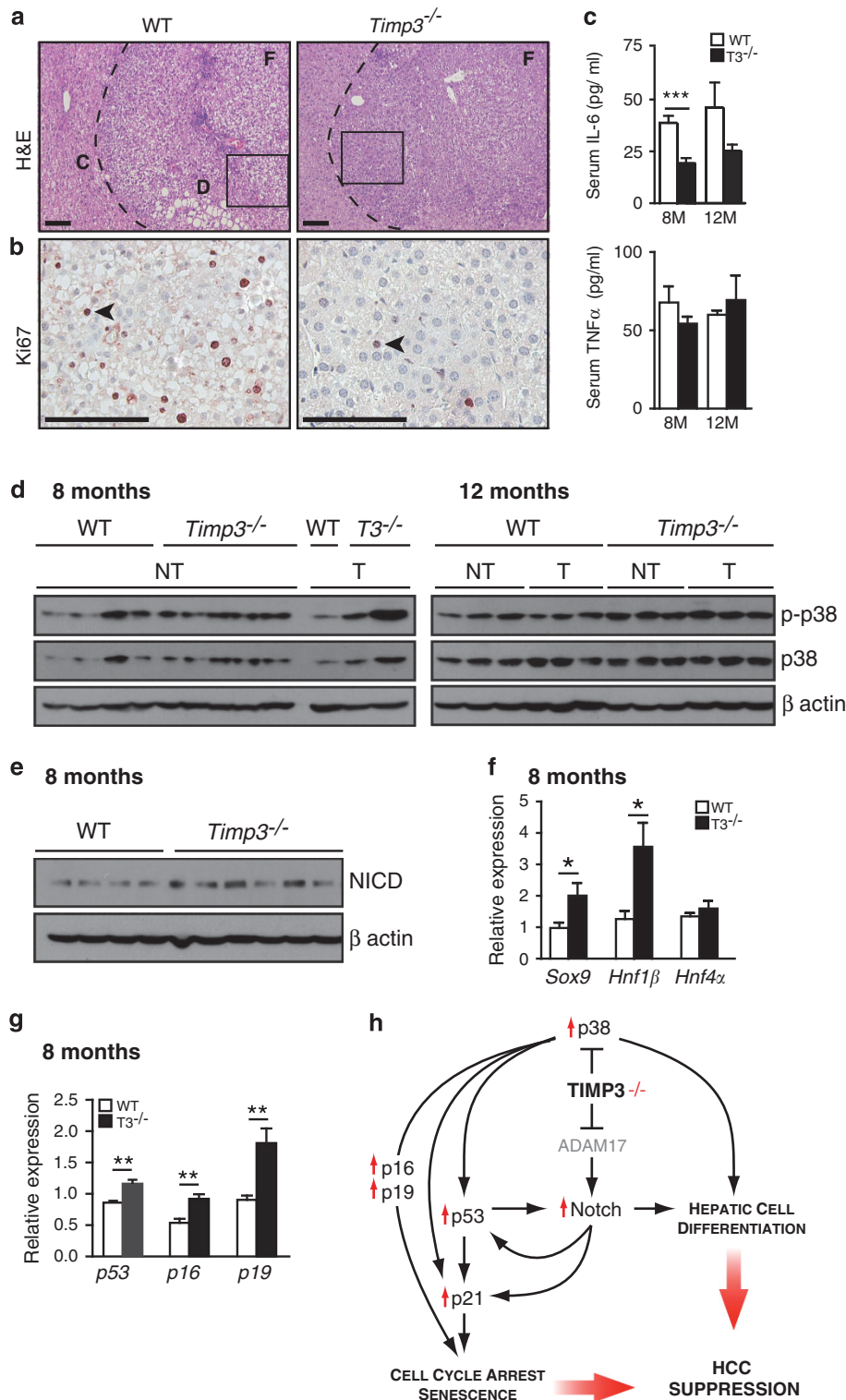


Figure 7. Comparative p38 and Notch activation in preneoplastic livers. **(a)** Characterization of the DEN-induced hepatic foci (F) at 8 months following DEN treatment (5 μg/g). Hematoxylin and eosin-stained liver sections showing WT foci with hepatic cell degeneration (D) and compression of adjacent normal hepatic parenchyma (C). **(b)** Ki67 immunostaining highlights cell proliferation in WT and *Timp3*^{-/-} liver; arrowheads indicate Ki67-positive hepatocytes in the windows shown in **a**. Scale bars, 100 μm. **(c)** Serum enzyme-linked immunosorbent assay for IL-6 and TNFα at 8 months (M) (WT, *n* = 8; *Timp3*^{-/-}, *n* = 12) and 12 months post DEN (WT, *n* = 9; *Timp3*^{-/-}, *n* = 8). **(d)** Immunoblotting for p-p38 in extracts from liver tumor (T) and corresponding adjacent non-tumor (NT) tissues at 8 and 12 months. **(e)** Immunoblotting for NICD, each lane represents a mouse and reverse transcription PCR analysis for **(f)** hepatic cell markers and **(g)** p16, p19 and p53 in preneoplastic livers at 8 months post DEN (WT, *n* = 9; *Timp3*^{-/-}, *n* = 12 mice per group). Data are presented as the mean ± s.e.m. **P* < 0.05, ***P* < 0.01 and ****P* < 0.001 for the indicated comparisons. **(h)** Model for TIMP3 instructed molecular interactions that integrate p53 activation with MAPK and Notch pathways to impact hepatocyte senescence, hepatic cell fate and HCC resistance. ADAM17 has been added in gray as a potential intermediate in the Notch pathway activation.

tumorigenesis by enhancing liver inflammation and/or controlling cell fate. On the other hand, although TIMP3 regulates the TNF pathway during inflammatory response in the liver, its action on HCC does not operate through TNF.

Upon DNA damage, p53 induces a transient growth arrest to allow DNA repair. Alternatively, it promotes senescence or apoptosis in case of extensive DNA damage.^{38,39} p53-induced senescence has been responsible for protection against HCC even after tumor formation, as brief reactivation of endogenous p53 in p53-null hepatic tumors leads to complete regression by induction of cell senescence and tumor clearance by immune cells.⁴⁰ Our study reveals that acute DEN exposure induces a transient p53 activation and hepatocyte apoptosis in WT liver, while precocious p53 activation leads to senescence in *Timp3*^{-/-} liver; p53 expression is also higher at the attenuated preneoplastic stage in the null liver. In addition, carcinogen-exposed *Timp3*^{-/-} fibroblasts show reduced apoptosis as well as greater p21 expression and senescence, thereby suggesting a mechanism not restricted to hepatocyte. The powerful tumor suppressor p53 has been under scrutiny for decades, although factors that collaborate to increase p53 activity and determine a specific cell fate are less well understood. Figure 7h models how signaling pathways influenced by TIMP3 integrate to enhance p53 bioactivity and trigger senescence, cell differentiation and facilitate tumor suppression. Specific knockdowns or inhibitors of individual pathways can provide a deeper understanding of these interactions in future studies.

Two other major pathways, p38 and Notch, were activated in *Timp3*^{-/-} livers. p38 negatively regulates cell cycle progression facilitating DNA repair^{41,42} by inducing p21 or directly activating p53. Moreover, a tumor-suppressive function of p38 was suggested in the liver, as hepatocyte-specific p38 α knockouts have a greater DEN-induced ROS accumulation, JNK activation, liver damage, compensatory hepatocyte proliferation and enhanced hepatocarcinogenesis.^{5,43} We pinpoint sustained p38 activation during the DNA damage response and liver cancer attenuation in *Timp3*-deficient mice, which is in line with our previous observation of MAPK (Erk1/2 and JNK) regulation by the TIMP3/ADAM17 axis during Fas-induced fulminant hepatitis.⁹ Interestingly, a recent study has placed this axis downstream of p38 activation. ADAM17 phosphorylation by p38 led to dissociation of ADAM17 dimer from TIMP3 on the cell surface and allowed ADAM17 activity.⁴⁴ Our work suggests that p38 functions as a tumor suppressor in *Timp3*^{-/-} liver, likely mediating the negative regulation of hepatic cell cycle progression and induction of terminal differentiation.^{42,45,46}

The decision between growth arrest, senescence or apoptosis is believed to be determined by the appropriate qualitative status of p53. For instance p53 nuclear concentration or its phosphorylation status can modulate its target gene promoter affinity, thus modulating the transcriptional program and cellular response.⁴⁷ Incidentally, consistent with the altered p53 activation kinetics in *Timp3* null tissue upon DEN challenge was the increased expression of p21 and MDM2, but lower expression of PUMA and NOXA pro-apoptotic target genes. It is conceivable that in the WT liver, the p38 inhibition observed at 4 h post DEN under the control of normal TIMP3 may direct the p53 DNA damage response toward apoptosis. In contrast, at the onset of DNA damage, the lack of TIMP3 and the subsequent sustained p38 activation may modify p53 conformation and/or stabilization and critically shift hepatocyte cell fate toward senescence.

We have recently shown the requirement of ADAM17 for Notch activation in the adult skin where it maintains the barrier immunity.³⁰ Because of its ability to inhibit ADAM17, TIMP3 can putatively regulate Notch, yet physiological evidence for this capacity has been lacking. Notch and p53 are interconnected; p53 directly binds to the *Notch 1* promoter to induce its expression and Notch in turn can stimulate p53 transcription via derepression of RBP-Jk bound to the p53 gene.⁴⁸ For instance ultraviolet-B and

genotoxic exposure induces Notch1 expression in a p53-dependent manner in skin and cultured keratinocytes.^{49,50} Notch1 has also been identified as a key determinant of keratinocyte differentiation, promoting cell cycle arrest through p21 induction and commitment to differentiation.⁵¹ In the liver, the Notch pathway activation affects hepatocyte growth and differentiation during regeneration,⁵² and coordinates biliary cell fate and morphogenesis in a temporal- and dose-dependent manner during hepatic development.^{31,33} More recently, Notch 2 was shown to direct biliary reprogramming of adult hepatocytes.⁵³ Interestingly, Notch1 overexpression in HCC cells induces a G0/G1 cell cycle arrest by acting on cell cycle regulators, and induces apoptosis by altering the balance between p53 and the anti-apoptotic protein Bcl-2.⁶ A contradictory pro-tumorigenic role of Notch signaling in liver has emerged in recent studies related to its prolonged overexpression.^{54,55} In the current study, increased Notch signaling in *Timp3*^{-/-} liver is reflected as higher NICD cleavage, and increased Notch-dependent hepatic cell markers at baseline, at acute post DEN and at preneoplastic stage. We propose that Notch signaling, via p53 and p21 activation, couples enhanced cell cycle arrest and senescence with hepatic cell differentiation to inhibit tumorigenesis.

Metalloproteinases generally promote cancer progression with their tissue inhibitors acting to suppress tumor cell properties.⁵⁶ A number of studies have shown *TIMP3* silencing through promoter hypermethylation to be associated with poor prognosis in human cancers including kidney, brain, colon, lung and endometrium, again suggesting it as a tumor suppressor gene.^{16,17,57} We provide convincing evidence that TIMP3, a metalloproteinase inhibitor that normally controls liver inflammation, increases the predisposition to hepatic tumorigenesis. This work sheds light on the complexity of metalloproteinase biology revealing their role in DNA damage response and hepatic cell fate. A better understanding of the underpinnings of protease-mediated p53 response in normal and cancer cells may impact our ability to develop future cancer therapy.

MATERIALS AND METHODS

Animal genotypes, treatment and tissue collection

Experimental animal protocols and animal procedures were in accordance with the guidelines approved by the Canadian Council for Animal Care and the Animal Care Committee of the Ontario Cancer Institute. All mice used in this study were on a C57BL/6 background. *Tnf*^{-/-} and *Tnfr1*^{-/-} mice obtained from the Jackson Laboratory (Bar Harbor, ME, USA) were crossed with the previously described *Timp3*^{-/-} mice⁷ to generate *Timp3*^{-/-}*Tnf*^{-/-} and *Timp3*^{-/-}*Tnfr1*^{-/-} mice. In long-term studies, HCC was induced by intraperitoneally administration of 5 μ g/g of DEN (Sigma-Aldrich, Oakville, ON, Canada) in 15-day-old male mice. Animals were euthanized by CO₂ inhalation at 8, 12 or 15 months post-DEN treatment. Visible tumors and lesions on the liver surface were counted and measured with calipers. Half of the left lobe from mice not showing liver surface tumors, or one part of the larger tumors as well as adjacent non-tumor tissue on the same lobe was snap-frozen; the other parts and lobes were fixed in 4% paraformaldehyde overnight and subsequently were paraffin-embedded. Liver sections (5 μ m) were hematoxylin and eosin-stained and were analyzed by one pathologist who was blinded to the genetic background. In short-term studies, 4-week-old male WT and *Timp3* null mice were treated (intraperitoneally) with PBS (control) or with an acute dose of DEN at 100 μ g/g and euthanized at 4, 12, 24 and 48 h post treatment to assess the early DNA damage response and hepatic injury. One part of the left and median lobes were fixed in 4% paraformaldehyde overnight, one part of the same lobes snap-frozen in liquid nitrogen and a part of the left lobe was frozen in optimal cutting temperature compound and used to assess SA- β -gal activity.

TUNEL staining and IHC

Sections (5 μ m) from paraffin-embedded liver tissue, obtained within 48 h of PBS or DEN injection (100 mg/kg), were subjected to TUNEL staining according to manufacturer's instructions (ApoAlert DNA fragmentation kit; Clontech, Mountain View, CA, USA). The apoptotic (green nucleus cells)

were counted around the central veins at x40 magnification in at least 10 fields. The results are plotted as number of TUNEL-positive cells per central vein. For IHC, 4% paraformaldehyde-fixed paraffin-embedded tissue sections were de-paraffinized in xylene, gradually rehydrated in descending concentrations of ethanol and subsequently treated in Borg Decloaker antigen retrieval solution (pH 9) for 5 min at 125 °C and 10 s at 90 °C using a Decloaking chamber (Biocare Medical, Concord, CA, USA). Tissue sections were stained using Horseradish peroxidase (HRP) 3-amino-9-ethylcarbazole (AEC) tissue staining kit according to manufacturer's instructions (R&D Systems, Minneapolis, MN, USA). Primary antibodies used were anti-Ki67 (Thermo Scientific (SP6), Burlington, ON, Canada) 1:200 dilution, anti-cleaved caspase 3 (no. 9661, 1:50) and anti-p53 (no. 2524, 1: 1500; Cell Signaling Technology, Danvers, MA, USA), anti- γ H2AX (05-636, 1:200; Millipore, Temecula, CA, USA). Ki67-positive hepatocytes were scored in the entire liver sections at x40 magnification and results are plotted as number of Ki67-positive hepatocytes per field. Positive hepatocyte nuclei for p53 were scored around 10 comparable size central veins at x40 magnification and their number plotted as number of p53-positive hepatocyte per central vein.

Western blotting

RIPA extraction buffer containing 50 mM Tris-HCl, pH 7.4, 1% Triton X-100, 0.1% SDS, 1% sodium deoxycholate, 10 mM EDTA, 150 mM NaCl, 200 μ M Na₃VO₄, 50 mM NaF and an appropriate dilution of Complete Mini, EDTA-free protease inhibitor cocktail tablets (Roche, Laval, QC, Canada) was used to lyse all tissues and MEFs, the lysates were stored at -80 °C. Total liver protein was extracted by mortar and pestle homogenization of snap-frozen tissues. A quantity of 30–40 μ g of protein was loaded on SDS-polyacrylamide gel electrophoresis gels for western blotting. The following primary antibodies were used: anti-phosphorylated JNK (p-JNK, Thr183/Tyr185), anti-JNK, anti-phosphorylated p44/42 MAPK (p-ERK1/2, Thr202/Tyr204), anti-p44/42 MAPK (ERK1/2), anti-p38 MAPK, anti-phosphorylated p38 MAPK (p-p38, Thr180/Tyr182), anti-cleaved caspase 3, anti-p53, anti-cleaved Notch1 (Cell Signaling Technology, Beverly, MA, USA) and anti p21, anti- β -actin, anti-p16 (Santa Cruz Biotechnology Inc., Santa Cruz, CA, USA). HRP-conjugated secondary antibodies against rabbit or mouse were obtained from Cell Signaling Technology.

MEF isolation and treatment

Primary WT and *Timp3*^{-/-} MEFs were harvested from 13.5-day-old embryos as described in Sun *et al.*⁵⁸ Cells were cultured at 37 °C (5% CO₂) in Dulbecco's modified Eagle's medium containing 10% fetal bovine serum. All experiments were performed using early passage MEF cultures (passages 2–3); cells were seeded in six-well plates at a density of 2 \times 10⁵ cells/well and used for the experiment at 70% confluency. MEFs cells were treated with the alkylating agent MMS (Sigma-Aldrich, Oakville, ON, Canada) at 130 μ g/ml for 2 h at 37 °C. Control cells were incubated at 37 °C for 2 h in culture media without MMS. The cells were washed twice with PBS and either immediately harvested for protein and RNA extractions (noted 0 h) or incubated for additional time (1.5, 4, 24 and 48 h) in fresh Dulbecco's modified Eagle's medium 10% fetal bovine serum to allow cell to recover from DNA damage before lysis.

Senescence-associated- β galactosidase activity

MEFs were fixed and stained using the SA- β -gal staining kit from Cell Signaling (no. 9860) according to manufacturer's instructions. The cells were visualized using a bright-field microscope at x10 magnification. One image per quarter of each six well-plate was taken using the Infinity 2 camera and Infinity Capture software, and a representative picture was chosen from four images. Cryosections (10- μ m-thick) of mouse liver tissues preserved in optimal cutting temperature were also assessed for SA- β -gal activity using the same Cell Signaling kit.

Serum and tissue analysis

Blood was collected from mice by cardiac puncture upon sacrifice at indicated time points and serum was obtained from whole blood by centrifugation and frozen until analysis. Liver injury was determined by measuring serum ALT levels. TNF α and IL-6 enzyme-linked immunosorbent assay were performed on diluted mouse serums (1:20). TNF α , IL-6 and IFN γ were also measured in 200 μ g of total liver protein homogenates obtained for the western blotting analysis using enzyme-linked immunosorbent assay protocol as per manufacturer's instructions (R&D Systems).

RNA preparation and quantitative reverse transcription PCR

RNA was prepared from frozen liver tissue using TRIzol reagent (Invitrogen, Carlsbad, CA, USA) according to manufacturer's instructions. cDNAs were obtained using a first-strand cDNA synthesis protocol (qScript cDNA supermix, Quanta Biosciences, Gaithersburg, MD, USA). Gene expression was measured using SYBR Green reagent (Perfecta SYBR Green Supermix ROX, Dural, NSW, Australia) in a 7800HT Real-time PCR system (Applied Biosystems, Carlsbad, CA, USA). All gene expression levels were normalized to hypoxanthine-guanine phosphoribosyltransferase (HPRT) and the fold change measured relative to liver samples from WT PBS-treated mice for the short-term study or the WT samples from the 8 and 12 months cohorts, or the untreated control MEFs for the *in vitro* experiments. Amount of each product was calculated using the 2^{- $\Delta\Delta$ CT} method. Primer sequences are provided in Supplementary Table S1.

Statistical analysis

Statistical analysis was carried out using GraphPad Prism 4 software (La Jolla, CA, USA). Data are expressed as mean \pm s.e.m. Statistical significance was calculated with a Student's *t*-test and the data are expressed as mean \pm s.e.m. *P* < 0.05 was considered to be statistically significant.

CONFLICT OF INTEREST

The authors declare no conflict of interest.

ACKNOWLEDGEMENTS

We would like to thank Dr Paul Waterhouse and Dr Razqallah Hakem for their constructive criticism of the manuscript. This work was supported by grants from the Canadian Institutes of Health Research to RK. VD was supported by the Helena H Lam and Fondation pour la Recherche Médicale fellowships.

REFERENCES

- 1 El-Serag HB. Hepatocellular carcinoma. *New Engl J Med* 2011; **365**: 1118–1127.
- 2 Laurent-Puig P, Zucman-Rossi J. Genetics of hepatocellular tumors. *Oncogene* 2006; **25**: 3778–3786.
- 3 Coussens LM, Werb Z. Inflammation and cancer. *Nature* 2002; **420**: 860–867.
- 4 Farazi PA, DePinho RA. Hepatocellular carcinoma pathogenesis: from genes to environment. *Nat Rev Cancer* 2006; **6**: 674–687.
- 5 Hui L, Bakiri L, Mairhorfer A, Schweifer N, Haslinger C, Kenner L *et al.* p38alpha suppresses normal and cancer cell proliferation by antagonizing the JNK-c-Jun pathway. *Nat Genet* 2007; **39**: 741–749.
- 6 Qi R, An H, Yu Y, Zhang M, Liu S, Xu H *et al.* Notch1 signaling inhibits growth of human hepatocellular carcinoma through induction of cell cycle arrest and apoptosis. *Cancer Res* 2003; **63**: 8323–8329.
- 7 Mohammed FF, Smookler DS, Taylor SE, Fingleton B, Kassiri Z, Sanchez OH *et al.* Abnormal TNF activity in *Timp3*^{-/-} mice leads to chronic hepatic inflammation and failure of liver regeneration. *Nat Genet* 2004; **36**: 969–977.
- 8 Smookler DS, Mohammed FF, Kassiri Z, Duncan GS, Mak TW, Khokha R. Tissue inhibitor of metalloproteinase 3 regulates TNF-dependent systemic inflammation. *J Immunol* 2006; **176**: 721–725.
- 9 Murthy A, Defamie V, Smookler DS, Di Grappa MA, Horiuchi K, Federici M *et al.* Ectodomain shedding of EGFR ligands and TNFR1 dictates hepatocyte apoptosis during fulminant hepatitis in mice. *J Clin Invest* 2010; **120**: 2731–2744.
- 10 Fiorentino L, Vivanti A, Cavalera M, Marzano V, Ronci M, Fabrizi M *et al.* Increased tumor necrosis factor alpha-converting enzyme activity induces insulin resistance and hepatosteatosis in mice. *Hepatology* 2010; **51**: 103–110.
- 11 Menghini R, Menini S, Amoroso R, Fiorentino L, Casagrande V, Marzano V *et al.* Tissue inhibitor of metalloproteinase 3 deficiency causes hepatic steatosis and adipose tissue inflammation in mice. *Gastroenterology* 2009; **136**: 663–72 e4.
- 12 Black RA, Rauch CT, Kozlosky CJ, Peschon JJ, Slack JL, Wolfson MF *et al.* A metalloproteinase disintegrin that releases tumour-necrosis factor-alpha from cells. *Nature* 1997; **385**: 729–733.
- 13 Peschon JJ, Slack JL, Reddy P, Stocking KL, Sunnarborg SW, Lee DC *et al.* An essential role for ectodomain shedding in mammalian development. *Science* 1998; **282**: 1281–1284.
- 14 Wisniewska M, Goettig P, Maskos K, Belouski E, Winters D, Hecht R *et al.* Structural determinants of the ADAM inhibition by TIMP-3: crystal structure of the TACE-N-TIMP-3 complex. *J Mol Biol* 2008; **381**: 1307–1319.
- 15 Black RA. TIMP3 checks inflammation. *Nat Genet* 2004; **36**: 934–935.
- 16 Bachman KE, Herman JG, Corn PG, Merlo A, Costello JF, Cavenee WK *et al.* Methylation-associated silencing of the tissue inhibitor of metalloproteinase-3

- gene suggest a suppressor role in kidney, brain, and other human cancers. *Cancer Res* 1999; **59**: 798–802.
- 17 Catusas L, Pons C, Munoz J, Espinosa I, Prat J. Promoter hypermethylation contributes to TIMP3 down-regulation in high stage endometrioid endometrial carcinomas. *Histopathology* 2013; **62**: 632–641.
 - 18 Garofalo M, Di Leva G, Romano G, Nuovo G, Suh SS, Ngankeu A *et al*. miR-221&222 regulate TRAIL resistance and enhance tumorigenicity through PTEN and TIMP3 downregulation. *Cancer Cell* 2009; **16**: 498–509.
 - 19 Wang B, Hsu SH, Majumder S, Kutay H, Huang W, Jacob ST *et al*. TGFbeta-mediated upregulation of hepatic miR-181b promotes hepatocarcinogenesis by targeting TIMP3. *Oncogene* 2010; **29**: 1787–1797.
 - 20 Masson D, Rioux-Leclercq N, Fergelot P, Jouan F, Mottier S, Theoleyre S *et al*. Loss of expression of TIMP3 in clear cell renal cell carcinoma. *Eur J Cancer* 2010; **46**: 1430–1437.
 - 21 Nakamura M, Ishida E, Shimada K, Kishi M, Nakase H, Sakaki T *et al*. Frequent LOH on 22q12.3 and TIMP-3 inactivation occur in the progression to secondary glioblastomas. *Lab Invest* 2005; **85**: 165–175.
 - 22 Maeda S, Kamata H, Luo JL, Leffert H, Karin M. IKKbeta couples hepatocyte death to cytokine-driven compensatory proliferation that promotes chemical hepatocarcinogenesis. *Cell* 2005; **121**: 977–990.
 - 23 Verna L, Whysner J, Williams GM. N-nitrosodiethylamine mechanistic data and risk assessment: bioactivation, DNA-adduct formation, mutagenicity, and tumor initiation. *Pharmacol Ther* 1996; **71**: 57–81.
 - 24 Kang JS, Wanibuchi H, Morimura K, Gonzalez FJ, Fukushima S. Role of CYP2E1 in diethylnitrosamine-induced hepatocarcinogenesis *in vivo*. *Cancer Res* 2007; **67**: 11141–11146.
 - 25 Mah LJ, El-Osta A, Karagiannis TC. gammaH2AX: a sensitive molecular marker of DNA damage and repair. *Leukemia* 2010; **24**: 679–686.
 - 26 Vesselinovich SD, Mihailovich N. Kinetics of diethylnitrosamine hepatocarcinogenesis in the infant mouse. *Cancer Res* 1983; **43**: 4253–4259.
 - 27 Luedde T, Beraza N, Kotsikoros V, van Loo G, Nenci A, De Vos R *et al*. Deletion of NEMO/IKKgamma in liver parenchymal cells causes steatohepatitis and hepatocellular carcinoma. *Cancer Cell* 2007; **11**: 119–132.
 - 28 Pikarsky E, Porat RM, Stein I, Abramovitch R, Amit S, Kasem S *et al*. NF-kappaB functions as a tumour promoter in inflammation-associated cancer. *Nature* 2004; **431**: 461–466.
 - 29 Poehlmann A, Roessner A. Importance of DNA damage checkpoints in the pathogenesis of human cancers. *Pathol Res Pract* 2010; **206**: 591–601.
 - 30 Murthy A, Shao YW, Narala SR, Molyneux SD, Zuniga-Pflucker JC, Khokha R. Notch activation by the metalloproteinase ADAM17 regulates myeloproliferation and atopic barrier immunity by suppressing epithelial cytokine synthesis. *Immunity* 2012; **36**: 105–119.
 - 31 Zong Y, Panikkar A, Xu J, Antoniou A, Raynaud P, Lemaigre F *et al*. Notch signaling controls liver development by regulating biliary differentiation. *Development* 2009; **136**: 1727–1739.
 - 32 Antoniou A, Raynaud P, Cordi S, Zong Y, Tronche F, Stanger BZ *et al*. Intrahepatic bile ducts develop according to a new mode of tubulogenesis regulated by the transcription factor SOX9. *Gastroenterology* 2009; **136**: 2325–2333.
 - 33 Tchorz JS, Kinter J, Muller M, Tornillo L, Heim MH, Bettler B. Notch2 signaling promotes biliary epithelial cell fate specification and tubulogenesis during bile duct development in mice. *Hepatology* 2009; **50**: 871–879.
 - 34 Cressman DE, Greenbaum LE, DeAngelis RA, Ciliberto G, Furth EE, Poli V *et al*. Liver failure and defective hepatocyte regeneration in interleukin-6-deficient mice. *Science* 1996; **274**: 1379–1383.
 - 35 Iyoda K, Sasaki Y, Horimoto M, Toyama T, Yakushijin T, Sakakibara M *et al*. Involvement of the p38 mitogen-activated protein kinase cascade in hepatocellular carcinoma. *Cancer* 2003; **97**: 3017–3026.
 - 36 Naugler WE, Sakurai T, Kim S, Maeda S, Kim K, Elsharkawy AM *et al*. Gender disparity in liver cancer due to sex differences in MyD88-dependent IL-6 production. *Science* 2007; **317**: 121–124.
 - 37 Knight B, Yeoh GC, Husk KL, Ly T, Abraham LJ, Yu C *et al*. Impaired preneoplastic changes and liver tumor formation in tumor necrosis factor receptor type 1 knockout mice. *J Exp Med* 2000; **192**: 1809–1818.
 - 38 Vousden KH, Prives C. Blinded by the light: the growing complexity of p53. *Cell* 2009; **137**: 413–431.
 - 39 Lowe SW, Ceprero E, Evan G. Intrinsic tumour suppression. *Nature* 2004; **432**: 307–315.
 - 40 Xue W, Zender L, Miething C, Dickins RA, Hernando E, Krizhanovsky V *et al*. Senescence and tumour clearance is triggered by p53 restoration in murine liver carcinomas. *Nature* 2007; **445**: 656–660.
 - 41 Han J, Sun P. The pathways to tumor suppression via route p38. *Trends Biochem Sci* 2007; **32**: 364–371.
 - 42 Bulavin DV, Fornace AJ Jr. p38 MAP kinase's emerging role as a tumor suppressor. *Adv Cancer Res* 2004; **92**: 95–118.
 - 43 Sakurai T, He G, Matsuzawa A, Yu GY, Maeda S, Hardiman G *et al*. Hepatocyte necrosis induced by oxidative stress and IL-1 alpha release mediate carcinogen-induced compensatory proliferation and liver tumorigenesis. *Cancer Cell* 2008; **14**: 156–165.
 - 44 Xu P, Liu J, Sakaki-Yumoto M, Derynck R. TACE activation by MAPK-mediated regulation of cell surface dimerization and TIMP3 association. *Sci Signal* 2012; **5**: ra34.
 - 45 Dolado I, Nebreda AR. Regulation of tumorigenesis by p38aMAP kinase. In: F Posas, AR Nebreda (eds). *Topics in Current Genetics: Stress-Activated Protein Kinases*. Springer-Verlag: Berlin, Heidelberg, 2008, pp 99–128.
 - 46 Hui L, Bakiri L, Stepniak E, Wagner EF. p38alpha: a suppressor of cell proliferation and tumorigenesis. *Cell Cycle* 2007; **6**: 2429–2433.
 - 47 Lavin MF, Gueven N. The complexity of p53 stabilization and activation. *Cell Death Differ* 2006; **13**: 941–950.
 - 48 Boggs K, Henderson B, Reisman D. RBP-Jkappa binds to and represses transcription of the p53 tumor suppressor gene. *Cell Biol Int* 2009; **33**: 318–324.
 - 49 Yugawa T, Handa K, Narisawa-Saito M, Ohno S, Fujita M, Kiyono T. Regulation of Notch1 gene expression by p53 in epithelial cells. *Mol Cell Biol* 2007; **27**: 3732–3742.
 - 50 Mandinova A, Lefort K, Tommasi di Vignano A, Stonely W, Ostano P, Chiorino G *et al*. The FoxO3a gene is a key negative target of canonical Notch signalling in the keratinocyte UVB response. *EMBO J* 2008; **27**: 1243–1254.
 - 51 Rangarajan A, Talora C, Okuyama R, Nicolas M, Mammucari C, Oh H *et al*. Notch signaling is a direct determinant of keratinocyte growth arrest and entry into differentiation. *EMBO J* 2001; **20**: 3427–3436.
 - 52 Kohler C, Bell AW, Bowen WC, Monga SP, Fleig W, Michalopoulos GK. Expression of Notch-1 and its ligand Jagged-1 in rat liver during liver regeneration. *Hepatology* 2004; **39**: 1056–1065.
 - 53 Jeliakova P, Jors S, Lee M, Zimmer-Strobl U, Ferrer J, Schmid RM *et al*. Canonical Notch2 signaling determines biliary cell fates of embryonic hepatoblasts and adult hepatocytes independent of Hes1. *Hepatology* 2013; **57**: 2469–2479.
 - 54 Dill MT, Tornillo L, Fritzius T, Terracciano L, Semela D, Bettler B *et al*. Constitutive Notch2 signaling induces hepatic tumors in mice. *Hepatology* 2013; **57**: 1607–1619.
 - 55 Villanueva A, Alsinet C, Yanger K, Hoshida Y, Zong Y, Toffanin S *et al*. Notch signaling is activated in human hepatocellular carcinoma and induces tumor formation in mice. *Gastroenterology* 2012; **143**: 1660–1669 e7.
 - 56 Kessenbrock K, Plaks V, Werb Z. Matrix metalloproteinases: regulators of the tumor microenvironment. *Cell* 2010; **141**: 52–67.
 - 57 Zochbauer-Muller S, Fong KM, Virmani AK, Geradts J, Gazdar AF, Minna JD. Aberrant promoter methylation of multiple genes in non-small cell lung cancers. *Cancer Res* 2001; **61**: 249–255.
 - 58 Sun H, Gulbagci NT, Taneja R. Analysis of growth properties and cell cycle regulation using mouse embryonic fibroblast cells. *Methods Mol Biol* 2007; **383**: 311–319.

Supplementary Information accompanies this paper on the Oncogene website (<http://www.nature.com/onc>)